J|A|C|S COMMUNICATIONS

Published on Web 05/15/2009

# Synthesis of Unique Ultrathin Lamellar Mesostructured $CoSe_2$−Amine (Protonated) Nanobelts in a Binary Solution

Min-Rui Gao, Wei-Tang Yao, Hong-Bin Yao, and Shu-Hong Yu*

*Division of Nanomaterials and Chemistry, Hefei National Laboratory for Physical Sciences at Microscale, Department of Chemistry, University of Science and Technology of China, Hefei, Anhui 230026, The People's Republic of China*

Received January 22, 2009; E-mail: shyu@ustc.edu.cn

Inorganic−organic hybrid composites aroused a lot of recent interest from the viewpoints of both new properties and technological applications.[1] Incorporation of two counterparts into a single structure may enhance or combine the superior electronic, magnetic, and optical feathers, rigidity, and thermal stability of inorganic frameworks with the structural diversity, flexibility, processability, and geometrical controllability of organic molecules. Recent advances show that novel hybrid II−VI semiconductors can be synthesized by incorporating segments (e.g., a slab or chain) of a II−VI semiconductor, MQ, and organic spacers (L) in one structure via coordinate or convalent bonds.[2] These structures have a composition of $[MQ(L)_x]$ (M = Mn, Zn, Cd; Q = S, Se, Te; L = mono- or diamine or hydrazine; $x = 0.5$ or 1.0), wherein nanometer-sized components of identical size are arranged in a perfectly periodic crystal structure.[2,3] In addition, many literature reports describe the preparation of 1D inorganic−organic hybrid nanocrystals,[4] e.g., ZnSe(diethylenetriamine)$_{0.5}$ nanobelts,[4a] $ZnS/N_2H_4$,[4b] ZnS/cyclohexylamine,[4c] ZnS/amine,[4d] $WO_{2.72}(N_6C_{123}H_{136}O_{22})_{0.04}$,[4e] $GeO_x$/ethylenediamine nanowires,[4f] and $Fe_{18}S_{25}$(triethylenetetramine)$_{14}$ nanoribbons,[4g] because of their potential applications as building blocks for electronic and optical nanodevices. Since the first discovery of mesoporous silica in 1992,[5] numerous systems of mesoporous metal oxides[6] and porous semiconductors[7] have been reported so far. Only a few studies, however, have been focused toward synthesizing a semiconductor and its organic mesostructured composites, such as Ge,[8] $GeS_2$, $SnS_2$, CdS, and CdSe.[9] Additionally, how to synthesize a mesostrucured composite with a well-defined shape has been rarely reported.

As an important pyrite-type compound, $CoSe_2$ is known as a metallic conductor and exchange-enhanced Pauli paramagnent in its ground state with a Curie temperature, $T_c$, of 124 K.[10] However, the extraordinary capability of $CoSe_2$ has rarely been researched in nanoscale materials primarily due to the limited availability of high-quality materials. Herein, we report a simple method for direct synthesis of the first mesostructed $CoSe_2$-amine (protonated) nanobelts (amine = diethylenetriamine (DETA), triethylenetetramine (TETA), and tetraethylenepentamine (TEPA)) in a binary solution under solvothermal conditions.

The $CoSe_2$-amine (protonated) composite nanobelts were synthesized by solvothermal reaction of $Co(Ac)_2 \cdot H_2O$ and $Na_2SeO_3$ in a mixed solution (40 mL) with a volume ratio of $V_{DETA}/V_{DIW} = 2:1$ (DIW = deionzed water) at 180 °C for 16 h (see Supporting Information, SI). The powder X-ray diffraction (XRD) of the samples was recorded in a $2\theta$ range of 3°−70°. The peaks of $00l'$ can be indexed as (001) and (002) with lattice spacings of 1.10 and 0.55 nm, respectively (Figure 1a). The other wide-angle reflections can be readily indexed to a pure primitive cubic phase of $CoSe_2$ structure with a lattice parameter of $a = 0.586$ nm (JCPDS 9-234). The broadening width of all reflections and the disappearance of some reflections should be related to the very thin layered structure of the obtained product.[11] Energy dispersive X-ray spectrum (EDS) analysis shows the mean atom ratio of Co/Se is 1:2 (SI, Figure S1). A room temperature Raman spectrum of the sample also confirms the formation of a cubic $CoSe_2$ phase[12] (SI, Figure S2).

Scanning electron microscopy (SEM) images in Figure 2a indicate that the sample is composed of nanobelts with widths of 100−500 nm and lengths up to several tens of micrometers. The transmission electron microscopy (TEM) image in Figure 2b shows that the nanobelts are flexible, smooth, thin, and almost transparent. The selected-area electron diffraction (SAED) pattern taken on a typical nanobelt shows the single-crystalline nature. The corresponding high-resolution TEM image in Figure 2d shows resolved lattice fringes of (210) planes with a spacing of 2.68 Å, which depicts that the growth direction is [210].

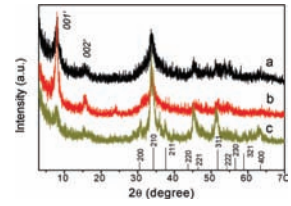


***Figure 1.*** XRD patterns of the samples prepared at 180 °C for 16 h in different binary solution. (a) $CoSe_2$-DETA nanobelts, $V_{TETA}/V_{DIW} = 2:1$. (b) $CoSe_2$-TEPA nanobelts, $V_{TEPA}/V_{DIW} = 2:1$. (c) $CoSe_2$-TETA nanobelts, $V_{TETA}/V_{DIW} = 2:1$.

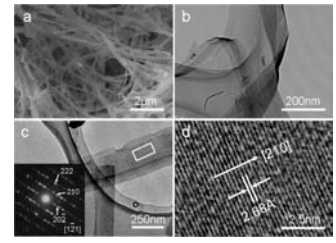


***Figure 2.*** (a, b) SEM and TEM images of the morphology of lamellar mesostructured $CoSe_2$-DETA nanobelts, respectively. (c) HRTEM image of a single lamellar mesostructured $CoSe_2$-DETA nanobelt. Inset shows the corresponding SAED pattern. (d) A typical HRTEM image taken on the marked part in (c).

Similarly, substitution of DETA by TETA and TEPA in $CoSe_2$-DETA (protonated) can also generate $CoSe_2$-TETA and $CoSe_2$-TEPA nanobelts with single crystal structures (Figure 1b,c, and SI, Figure S3). It should be noted that the $CoSe_2$-TETA (or TEPA) mesostructured nanobelts have almost the same interlamellar distances with that for $CoSe_2$-DETA nanobelts.

Interestingly, a lateral view of the as-obtained nanobelts along the thickness direction clearly shows well-defined multilayered


10.1021/ja900506x CCC: $40.75 

nanostructures, and the direction of the strips is parallel to the [210] direction (Figure 3). The interlayer distance can be estimated to be ~1.08 nm, which is in good agreement with that detected by XRD. It is worth noting that the observed thickness of a single $CoSe_2$ layer is ~0.57 nm which is equal to its lattice parameter (Figure 3c). To the best of our knowledge, this kind of multilayered mesostructured nanobelt is totally different from other mesostructured 1D nanomaterials obsersed previously.[4d,f]

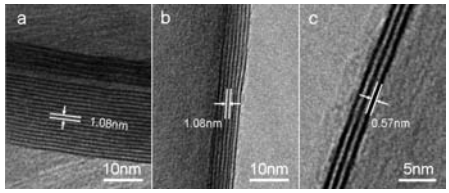


***Figure 3.*** (a−c) Typical HRTEM images viewed along the lateral thickness direction, which were taken on individual nanobelts.

***Scheme 1.*** Formation of $CoSe_2$-DETA Mesostructured Nanobelts[a]

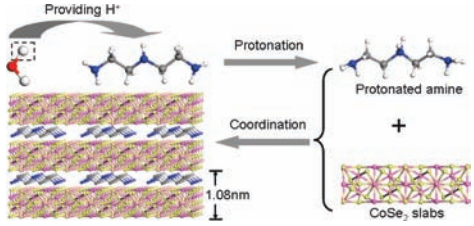


[a] The proposed formation mechanism of the $CoSe_2$-DETA mesostructured nanobelts. Red, white, blue, gray, pink, and yellow balls correspond to O, H, N, C, Co, and Se atoms, respectively. Hydrogen atoms are omitted for clarity in the structure.

An FT-IR spectrum shows that the vibration bands of $-CH_2-$, $-NH_2$, C−N, and −NH suggest the existence of DETA in the product (SI, Figure S4). Compared with that of pure DETA, the weak intensity of all vibrations and the absence of several bands presumably are due to the rather low content of DETA in the hybrid structure. The binding energy of N1s is identified at 400.5 eV, which is close to the binding energy of protonated amine (401.1 eV)[13] and also suggests the presence of DETA in the product (SI, Figure S5). X-ray fluorescence (XRF) analysis further confirms the existence of the low content of DETA in the product (SI, Figure S6). Thermal gravimetric analysis (TGA) shows that ~4.2 wt % DETA remained in the sample (SI, Figure S7). Removal of the amine at elevated temperature will result in the formation of pure phase $CoSe_2$ nanobelts (SI, Figure S8).

The influence of reaction time and temperature on the formation of such mesostructures and morphology has been carefully investigated. Well-defined $CoSe_2$-DETA (protonated) mesostructured nanobelts can only be obtained in a mixed solvent within a very narrow volume ratio range of $V_{DETA}/V_{DIW}$ (SI, Table S1, Figures S9, S10). Increasing the volume ratio of $V_{DETA}/V_{DIW}$ up to 2:5 or 1:6 will result in the formation of a pure $CoSe_2$ phase only. The favorable conditions for the formation of such nanobelts are to initiate the reaction at 180 °C for 16 h in a mixed solvent with a volume ratio of $V_{DETA}/V_{DIW} = 2:1$.

The formation mechanism of the above unique mesostructured nanobelts has been proposed in Scheme 1. First, some amine molecules used here are protonated by reaction with water under solvothermal conditions at 180 °C and form positively charged ammonium ions. Then, the protonated amine molecules are incorporated into neighboring $CoSe_2$ layers by coordination with Se. Here, the amine with a linear configuration acts as a template molecule, which not only leads to the new mesostructured nanobelts but also induces anisotropic growth of 1D nanostructures. This is analogous to the so-called solvent coordination molecular template mechanism.[14] Furthermore, the interlamellar distances still keep constant although other amines with different chain lengths were used, because the protonated amine molecules are incorporated into the inorganic framework by taking a horizontal configuration from the viewpoint of energy minimization (SI, Figure S11). The experiments showed that the $CoSe_2$-DETA nanobelts are stable in pure acetic acid but not stable in week alkali solution, which can further confirm that the occurrence of protonation of amine molecules played a key role in the formation of such mesostructures (SI, Figures S12, S13).

In summary, unique ultrathin $CoSe_2$-amine (protonated) mesostructured nanobelts with multiple stacked layers which are highly parallel to the axial direction have been first prepared in a binary solution of organic amine and water under mild solvothermal conditions. This synthesis strategy may open new avenues toward the syntheses of other mesostructured nanomaterials with unique shapes and structural features, which may bring new nontrivial functionalities.

**Acknowledgment.** This work was supported by the NSFC (50732006, 20621061, 20671085, 20701035), 2005CB623601, and the Partner Group of the CAS-MPG.

**Supporting Information Available:** Preparation procedures and characterization, and TEM, XRD, HRTEM, FT-IR. This material is available free of charge via the Internet at http://pubs.acs.org.

## References

(1) (a) Sanchez, C.; Lebeau, B.; Chaput, F.; Boilot, J. P. *Adv. Mater.* **2003**, *15*, 1969. (b) Sanchez, C.; Julián, B.; Belleville, P.; Popall, M. *J. Mater. Chem.* **2005**, *15*, 3559. (c) Yao, W. T.; Yu, S. H. *Adv. Funct. Mater.* **2008**, *18*, 3357.
(2) (a) Huang, X. Y.; Li, J.; Fu, H. X. *J. Am. Chem. Soc.* **2000**, *122*, 8789. (b) Heulings, H. R.; Huang, X. Y.; Li, J.; Yuen, T.; Lin, C. L. *Nano Lett.* **2001**, *1*, 521. (c) Huang, X. Y.; Li, J. *J. Am. Chem. Soc.* **2007**, *129*, 3157. (d) Yu, S. H.; Yoshimura, M. *Adv. Mater.* **2002**, *14*, 296.
(3) (a) Huang, X. Y.; Li, J.; Zhang, Y.; Mascarenhas, A. *J. Am. Chem. Soc.* **2003**, *125*, 7049. (b) Huang, X. Y.; Heulings, H. R.; Le, V.; Li, J. *Chem. Mater.* **2001**, *13*, 3754.
(4) (a) Yao, W. T.; Yu, S. H.; Huang, X. Y.; Jiang, J.; Zhao, L. Q.; Pan, L.; Li, J. *Adv. Mater.* **2005**, *17*, 2799. (b) Dong, Y. J.; Peng, Q.; Li, Y. D. *Inorg. Chem. Comm.* **2004**, *7*, 370. (c) Fan, L. B.; Song, H. W.; Zhao, H. F.; Pan, G. H.; Yu, H. Q.; Bai, X.; Li, S. W.; Lei, Y. Q.; Dai, Q. L.; Qin, R. F.; Wang, T.; Dong, B.; Zheng, Z. H.; Ren, X. G. *J. Phys. Chem. B* **2006**, *110*, 12948. (d) Yao, W. T.; Yu, S. H.; Wu, Q. S. *Adv. Funct. Mater.* **2007**, *17*, 623. (e) Polleux, J.; Pinna, N.; Antonietti, M.; Niederberger, M. *J. Am. Chem. Soc.* **2005**, *127*, 15595. (f) Gao, Q. S.; Chen, P.; Zhang, Y. H.; Tang, Y. *Adv. Mater.* **2008**, *20*, 1837. (g) Zang, Z. A.; Yao, H. B.; Zhou, Y. X.; Yao, W. T.; Yu, S. H. *Chem. Mater.* **2008**, *20*, 4749.
(5) Kresge, C. T.; Leonowicz, M. E.; Roth, W. J.; Vartuli, J. C.; Beck, J. S. *Nature* **1992**, *359*, 710.
(6) Yang, P. D.; Zhao, D. Y.; Margolese, D. I.; Chmelka, B. F.; Stucky, G. D. *Nature* **1998**, *396*, 152.
(7) (a) Mohanan, J. L.; Arachchige, I. U.; Brock, S. L. *Science* **2005**, *307*, 397. (b) Bag, S.; Trikalitis, P. N.; Chupas, P. J.; Armatas, G. S.; Kanatzidis, M. G. *Science* **2007**, *317*, 490.
(8) Armatas, G. S.; Kanatzidis, M. G. *Science* **2006**, *313*, 817.
(9) (a) Maclachlan, M. J.; Coombs, N.; Ozin, G. A. *Nature* **1999**, *397*, 681. (b) Scott, R. W. J.; Maclachlan, M. J.; Ozin, G. A. *Curr. Opin. Solid State Mater. Sci.* **1999**, *4*, 113. (c) Braun, P. V.; Osenar, P.; Stupp, S. I. *Nature* **1996**, *380*, 325. (d) Neeraj.; Rao, C. N. R. *J. Mater. Chem.* **1998**, *8*, 279.
(10) (a) Sato, H.; Nagasaki, F.; Kani, Y.; Senba, S.; Ueda, Y.; Kimura, A.; Taniguchi, M. *Solid State Commun.* **2001**, *118*, 563. (b) Waki, S.; Kasai, N.; Ogawa, S. *Solid State Commun.* **1982**, *41*, 835. (c) Inoue, N.; Yasuoka, H. *Solid State Commun.* **1979**, *30*, 341.
(11) Polleux, J.; Antonietti, M.; Niederberger, M. *J. Mater. Chem.* **2006**, *16*, 3969.
(12) Campos, C. E. M.; de Lima, J. C.; Grandi, T. A.; Machado, K. D.; Pizani, P. S. *Physica B* **2002**, *324*, 409.
(13) Nakayama, M.; Hoyashita, R.; Komatsu, H.; Muneyama, E.; Shoda, K.; Kunishige, A. *Langmuir* **2007**, *23*, 3462.
(14) Li, Y. D.; Liao, H. W.; Ding, Y.; Fan, Y.; Zhang, Y.; Qian, Y. T. *Inorg. Chem.* **1999**, *38*, 1382.

JA900506X